## scientific reports



### **OPEN**

# Finite element analysis of the modified intramedullary nail-II for managing reverse obliquity trochanteric fractures

Qian Wang, Yao Lu, Lu Liu, Teng Ma, Zhong Li, Kun Zhang<sup>™</sup> & Qiang Huang<sup>™</sup>

Cephalomedullary nails are widely used to fix unstable femoral trochanteric fractures nowadays. However, for reverse obliquity trochanteric (ROT) fractures, the fixation failure rate of existing cephalomedullary nails is high, resulting in many complications. Our team aimed to propose the modified intramedullary nail-II (MIN-II) to improve the fixation effects of ROT fractures and make biomechanical comparisons between MIN-II and three other cephalomedullary nails by finite element method. AO/OTA 31-A3.1 and 31-A3.3 ROT fracture models were established via a series of femoral CT data. Four cephalomedullary nails were constructed, including MIN-II, proximal femoral bionic nail (PFBN), InterTAN nail (ITN), and proximal femoral nail antirotation (PFNA). Then, these implants were assembled onto the above ROT fracture models. After setting boundary conditions, the mesh convergence test and model validation were performed. The evaluation indicators comprised von Mises stress (VMS) and displacement. To compare the mechanical stability of four implants, the percent difference (PD) was calculated. The values of maximal VMS on implants were 176.81 MPa, 292.04 MPa, 227.36 MPa, and 306.45 MPa in 31-A3.1 ROT fracture and 257.32 MPa, 349.90 MPa, 372.93 MPa, and 679.75 MPa in 31-A3.3 ROT fracture for the MIN-II, PFBN, ITN, and PFNA models under axial loads of 2100 N. Compared to the PFNA model, the PD reduction of MIN-II was 42.3% in 31-A3.1 ROT fracture and 62.1% in 31-A3.3 ROT fracture. The values of maximal displacement were 14.38 mm, 18.95 mm, 18.86 mm, and 20.53 mm in 31-A3.1 ROT fracture and 16.40 mm, 19.02 mm, 19.21 mm, and 20.56 mm in 31-A3.3 ROT fracture for the MIN-II, PFBN, ITN, and PFNA models. In comparison with the PFNA group, the MIN-II group showed a 30.0% reduction in 31-A3.1 ROT fracture and a 20.2% reduction in 31-A3.3 ROT fracture for this indicator, respectively. The values of maximal VMS on bones and maximal displacement of fracture surface exhibited similar trends for the four fixation groups. The modified intramedullary nail-II displayed the best biomechanical stability among the four cephalomedullary nails for the management of reverse obliquity trochanteric fractures. Hence, the MIN-II might be a good option for patients with ROT fractures.

Keywords Reverse obliquity, Modified, Finite element, Stability, Cephalomedullary, Fracture, Biomechanical

Reverse obliquity trochanteric (ROT) fractures account for up to 20% of all femoral trochanteric fractures¹. It mainly occurs in elderly patients, especially those with osteoporosis. According to the AO/OTA fracture and dislocation classification, this type of fracture is classified as AO/OTA 31-A3 (31-A3)². The typical characteristic of ROT fractures is the direction of the main fracture line, which is from distal-lateral to proximal-medial or approximately horizontal¹. Unlike 31-A1 and 31-A2 fractures, in 31-A3 fractures both the medial and lateral walls of the proximal femur are involved. These features of 31-A3 fractures make them own different biomechanical characteristics. Scholars have reached a consensus on early surgical treatment for such fractures³.⁴. Unfortunately, the surgical failure rate for ROT fractures is high, and there are many postoperative complications, such as screw cut-out, screw withdrawal, varus deformity, peri-implant fracture, screw breakage, etc.⁵-7. These not only seriously affect the rehabilitation process of elderly patients, but also bring great trouble to them and increase the mortality rate. Therefore, ROT fractures have been a thorny issue faced by orthopedic surgeons.

Due to the large trauma and high failure rate, the application of extramedullary fixation devices in ROT fractures is gradually decreasing, including dynamic hip screw, proximal femoral locking plates, etc. Conversely,

Department of Orthopedics, Honghui Hospital, Xi'an Jiaotong University, Xi'an 710054, Shaanxi, China. <sup>™</sup>email: qukezhangk@163.com; 369292735@qq.com

cephalomedullary nails have been used as the gold standard for the treatment of femoral trochanteric fractures, such as PFNA<sup>8,9</sup>. Cephalomedullary nails belong to the central fixation devices, which has a shorter lever arm compared to extramedullary fixation devices. This is beneficial for local stress dispersion. In addition, after satisfactory reduction, these cephalomedullary nails can usually be implanted via a minimally invasive method. This helps protect the local circulation. Despite these advantages, for ROT fractures, the head screws of these cephalomedullary nails (PFNA, ITN, and Gamma3 nail) are almost parallel to the main fracture line. In this case, it is easy to cause complications such as femoral shaft internalization and head screw cut-out, resulting in a high failure rate of fixation 5-7. PFBN is a cephalomedullary nail designed based on the theory of triangular stability and lever balance<sup>10</sup>. Some clinical and biomechanical studies have shown that PFBN was more effective than the PFNA in fixing femoral trochanteric fractures<sup>10,11</sup>. Other studies indicated that PFBN had better biomechanical stability than PFNA and ITN in fixing ROT fractures<sup>12,13</sup>. Yet, although the PFBN device has two head screws (the tension and pressure screws), it faces a similar issue in fixing ROT fractures. The angles between the head screws and the main fracture line present small acute angles. Both head screws of PFBN are located on the same side of the main fracture line, which has a limited effect on restricting sliding of the fracture fragments. Cerclage cable technique can indeed enhance the local mechanical stability of the fracture site for ROT fractures<sup>14</sup>. However, scholars have to face the risks of significant trauma, excessive bleeding, and increased postoperative infections when applying cerclage cable technique. So far, there is no specially designed cephalomedullary nails for fixing ROT fractures in clinical work.

Given the current situation, our team designed the modified intramedullary nail-II (MIN-II, Fig. 1A) to treat reverse obliquity trochanteric fractures. In our previous research, the MIN device has been proven to be effective in fixing 31-A2.3 femoral trochanteric fractures<sup>15</sup>. Compared to the MIN, the MIN-II has undergone minor optimization to better fix ROT fractures. In MIN-II, two head screws are fixed to the femoral head along the femoral neck after passing through the main nail. These two head screws are arranged in parallel. The interlocking screw is locked at a right angle with the tail of the lower head screw, and finally fixed to the area below the lesser trochanter. The main nail, the lower head screw, and the interlocking screw form a small triangular stable structure. Our team hoped that the MIN-II, with its unique design, would bring superior fixation and good stability for ROT fractures.

Finite element analysis (FEA) is a modern computational method based on structural mechanics analysis. This method was first applied in the field of mechanics in the 1950s. Currently, it is widely used in verifying the reliability and safety of new implants. By analyzing the stress, strain, displacement and other parameters of new implants under different load conditions, researchers could optimize the design and improve the biomechanical properties. In this research, four fixation models were constructed by FEA, including MIN-II, PFBN, ITN, and PFNA. Two ROT fracture models (AO/OTA 31-A3.1 and 31-A3.3) were established. The evaluation indicators comprised maximal VMS and displacement. Through these mechanical evaluation and comparison, our team attempted to preliminarily clarify the effects of MIN-II in fixing ROT fractures.

#### Materials and methods Three-dimensional (3D) building of ROT fractures

Written informed consents have been gotten from the volunteers, and all methods were conducted according to relevant guidelines and regulations. The experimental protocol has been approved by the ethics committee of Xi'an Honghui Hospital. For these volunteers, the exclusion criteria included severe osteoporosis, limb deformities, bone tumors, etc. Preliminary screening comprised X-ray and bone density examination. Then, CT data of the left femur were obtained from 20 volunteers. On the basis of the mean CT values, a standard 3D femur model was built by the Mimics (Materialize Co., Leuven, Belgium). For smoothing and surface fitting, the femoral model was saved as a STL file and imported into Studio (Geomagic Co., US). To differentiate cortex and cancellous bones, Hounsfield Unit (HU) was introduced 16. According to previous acknowledged fracture map and the 2018 AO/OTA Classification 2.17, two ROT fractures (AO/OTA 31-A3.1 and 31-A3.3) were constructed (Fig. 1E,F).

#### Construction of four fixation models and mesh convergence test

In computer-aided design (CAD) (Autodesk Co., US), four implants (MIN-II, PFBN, ITN, and PFNA, Fig. 1A–D) were designed according to the parameters provided by the manufacturer and our team. Then, these implants were installed on the ROT fracture models. The length of the four cephalomedullary nails was 240.0 mm while the diameter of the main nails was 10.0 mm. For the MIN-II, the diameters of two head screws and the interlocking screw are set as 10.0 mm, 5.0 mm, and 5.0 mm. The intersection angle between the main nail and the lower head screw is defined as 130°. Moreover, the intersection angle between the lower head screw and the interlocking screw is exactly at a right angle. The mesh type of this research was determined as tetrahedral elements during finite element modelling. Referring to similar researches, a mesh convergence test of these fixation models was carried out to assess the reliability<sup>18,19</sup>. 1.5 mm has been determined as the mesh size for this study. For maximal degree of freedom, field variables, comprising strain energy and displacement, were within the scope of 5% for both types of elements and there was no maximum stress point. Based on these results, our finite element models were proven to be reliable.

#### Material properties and boundary situation

According to previous researches, the material properties of these finite element models were set uniformly as homogeneous, isotropic, and linear elastic  $^{20}$ . The metal property of these cephalomedullary nails was determined as Titanium alloy. Based on similar researches, the parameter settings for Young's modulus and Poisson's ratio are listed in Table  $1^{21}$ . The values of elements and nodes for four fixation groups are displayed in Table 2. The type of contact between bones, cephalomedullary nails, and fracture fragments was defined as frictional contact. The

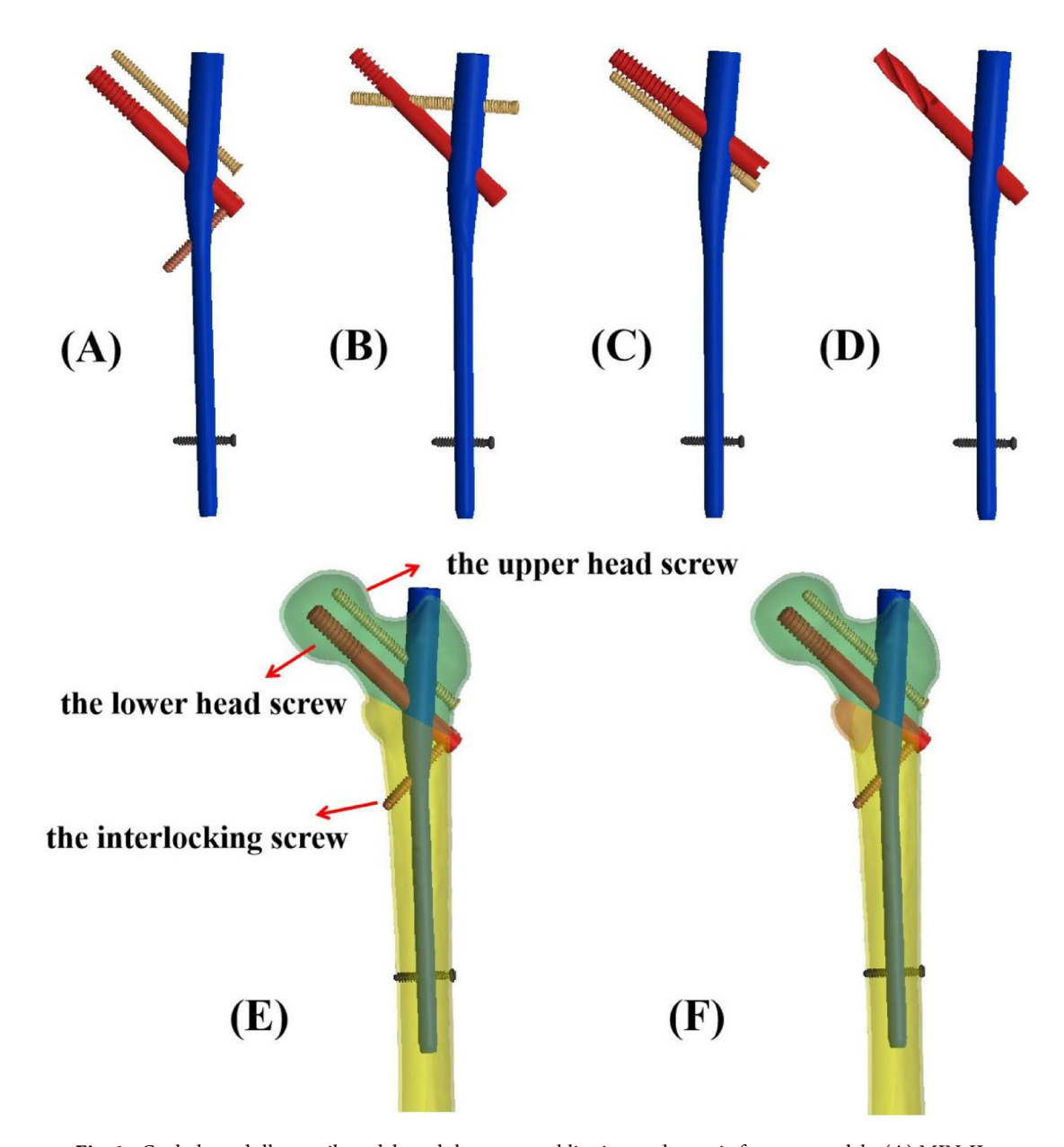


**Fig. 1.** Cephalomedullary nail models and the reverse obliquity trochanteric fracture models. **(A)** MIN-II. **(B)** PFBN. **(C)** ITN. **(D)** PFNA. **(E)** The MIN-II in AO/OTA 31-A3.1 fracture model. **(F)** The MIN-II in AO/OTA 31-A3.3 fracture model. *MIN-II* modified intramedullary nail-II, *PFBN* proximal femoral bionic nail, *ITN* InterTAN nail, *PFNA* proximal femoral nail antirotation.

Material	Elastic modulus (MPa)	Poisson's ratio
Titanium alloy	105,000	0.35
Cancellous bones	840	0.2
Cortical bones	16,800	0.3

Table 1. Indicator settings of elastic modulus and Poisson's ratio.

frictional coefficient values for implant-implant, bone-bone, and bone-implant surfaces were defined as 0.2, 0.46, and 0.3, respectively<sup>22</sup>. In order to evaluate the effects of vertical compression, the distal femur of each finite element model was properly fixed. The abduction angle was set as 10° while the tilt-back angle was 9° for these femoral models. The workload was set to 2100 N acting onto the femoral head surface in the vertical direction<sup>23</sup>. Marc Mentat 2016 (MSC Co.,US) was adopted in our finite element analysis and the analysis was solved via an implicit solver.

	31-A3.1		31-A3.3	
Model	Elements	Nodes	Elements	Nodes
MIN-II	616,963	971,428	616,647	970,797
PFBN	602,061	953,041	600,984	951,307
ITN	614,065	966,612	610,530	960,512
PFNA	565,320	881,103	564,934	880,330

**Table 2**. Number of elements and nodes for the four groups. *MIN-II* modified intramedullary nail-II, *PFBN* proximal femoral bionic nail, *ITN* InterTAN nail, *PFNA* proximal femoral nail antirotation.

#### Observation indexes and model validation

The observation indexes included maximal VMS on implants and bones, maximal displacement, and maximal displacement of fracture surface (MDFS). As the PFNA device was widely used in managing femoral trochanteric fractures in the past few decades, it was defined as the control group in our research<sup>24</sup>. Inter-group comparison was presented using percent difference (PD) which was calculated on the basis of the following formula:  $PD = (P_1 - Pa)/P_1 \times 100\%^{22}$ . Pa indicates the results of the MIN-II, PFBN, or ITN while  $P_1$  indicates the result of PFNA.

To conduct model validation, a standard femoral model was constructed through finite element method. The material properties were the same as those set in our previous text. The distal femur was fixed and vertical loads of 2100 N were loaded onto the femoral head. Axial stiffness of the intact femur was evaluated by the Ansys19.0 (ANSYS, US) and compared with experimental results published in previous research<sup>25</sup>. After testing, the axial stiffness of the femoral model in our study was 0.58 kN/mm. This result was very close to the experimental values of  $[(0.76\pm0.26) \text{ kN/mm}]$  which has been published in previous research<sup>25</sup>. The VMS distribution increased gradually from the distal femur to the proximal femur. In the light of individual difference for each model, our finite element models were validated.

#### Results

#### Maximal von Mises stress on implants

The bar plots of maximal VMS on implants under axial loads of 2100 N are displayed in Fig. 2A while the cloud pictures of maximal VMS on implants for the four fixation groups are shown in Fig. 3. For 31-A3.1 fracture models, the maximal VMS on implants was 176.81 MPa, 292.04 MPa, 227.36 MPa, and 306.45 MPa for the MIN-II, PFBN, ITN, and PFNA groups. Besides, it was 257.32 MPa, 349.90 MPa, 372.93 MPa, and 679.75 MPa for these groups in 31-A3.3 fracture models. The results of maximal VMS on implants for the MIN-II groups were lower than those of the PFNA groups in two ROT fracture models. The PD reduction for the MIN-II group was 42.3% and 62.1% in 31-A3.1 and 31-A3.3 fracture models, compared with the PFNA group.

#### Maximal von Mises stress on bones

The bar plots of maximal VMS on bones are exhibited in Fig. 2B while the cloud pictures of maximal VMS on bones for these groups are presented in Fig. 4. The maximal VMS on bones was 90.52 MPa, 66.66 MPa, 81.11 MPa, and 217.58 MPa for the MIN-II, PFBN, ITN, and PFNA groups in 31-A3.1 fracture models. Moreover, it was 171.90 MPa, 188.89 MPa, 297.38 MPa, and 315.86 MPa in 31-A3.3 fracture models. The results of maximal VMS on bones for the MIN-II groups were lower than those of the PFNA groups in two ROT fracture models. Compared with the PFNA group, the PD reduction of this observation index for the MIN-II group was 58.4% and 45.6% in 31-A3.1 and 31-A3.3 fracture models.

#### Maximal displacement for the four fixation groups

For 31-A3.1 fracture models, the maximal displacement was 14.38 mm, 18.95 mm, 18.86 mm, and 20.53 mm for the MIN-II, PFBN, ITN, and PFNA groups under axial loads of 2100 N, respectively. The values were 16.40 mm, 19.02 mm, 19.21 mm, and 20.56 mm in 31-A3.3 fracture models for these fixation groups. Obviously, the results of maximal displacement for the MIN-II groups were smaller than those of the PFNA groups in two ROT fracture models. The PD reduction of this observation index for the MIN-II group relative to the PFNA group was 30.0% and 20.2% in 31-A3.1 and 31-A3.3 fracture models. The bar plots of maximal displacement for the four fixation groups are shown in Fig. 2C while the cloud pictures for these groups are displayed in Fig. 5.

#### MDFS for the four fixation groups

The MDFS was 12.01 mm, 13.32 mm, 13.73 mm, and 17.37 mm for the MIN-II, PFBN, ITN, and PFNA groups in 31-A3.1 fracture models under axial load case. Notably, it was 13.18 mm, 14.43 mm, 13.79 mm and 17.93 mm in 31-A3.3 fracture models for these fixation groups. The results of MDFS for the MIN-II groups were smaller than those of the PFNA groups in two ROT fracture models. The PD reduction of MDFS for the MIN-II group was 30.8% and 26.5% in 31-A3.1 and 31-A3.3 fracture models, compared with the PFNA group. The bar plots of MDFS for the four fixation groups are presented in Fig. 2D while the cloud images for these groups are exhibited in Fig. 6.

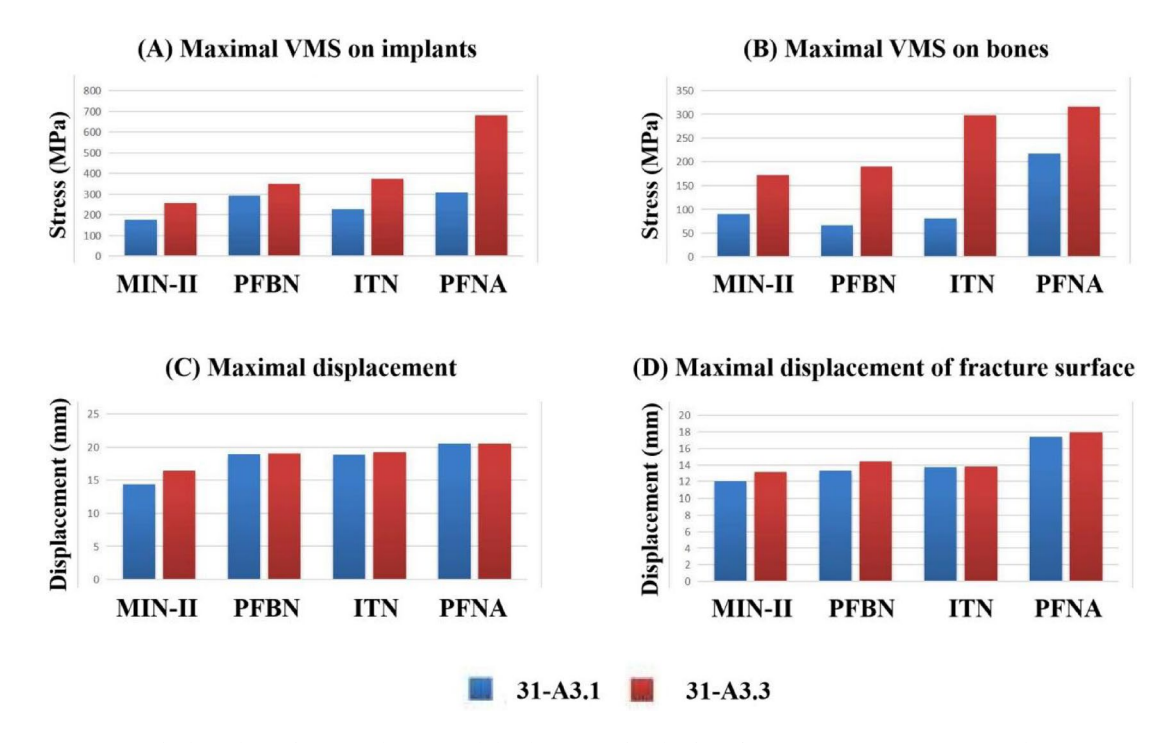


**Fig. 2.** The bar plots of maximal VMS and displacement for the four fixation groups in 31-A3.1 and 31-A3.3 fracture models. (**A**) Maximal VMS on implants. (**B**) Maximal VMS on bones. (**C**) Maximal displacement. (**D**) Maximal displacement of fracture surface. VMS represents von Mises stress. *MIN-II* modified intramedullary nail-II, *PFBN* proximal femoral bionic nail, *ITN* InterTAN nail, *PFNA* proximal femoral nail antirotation.

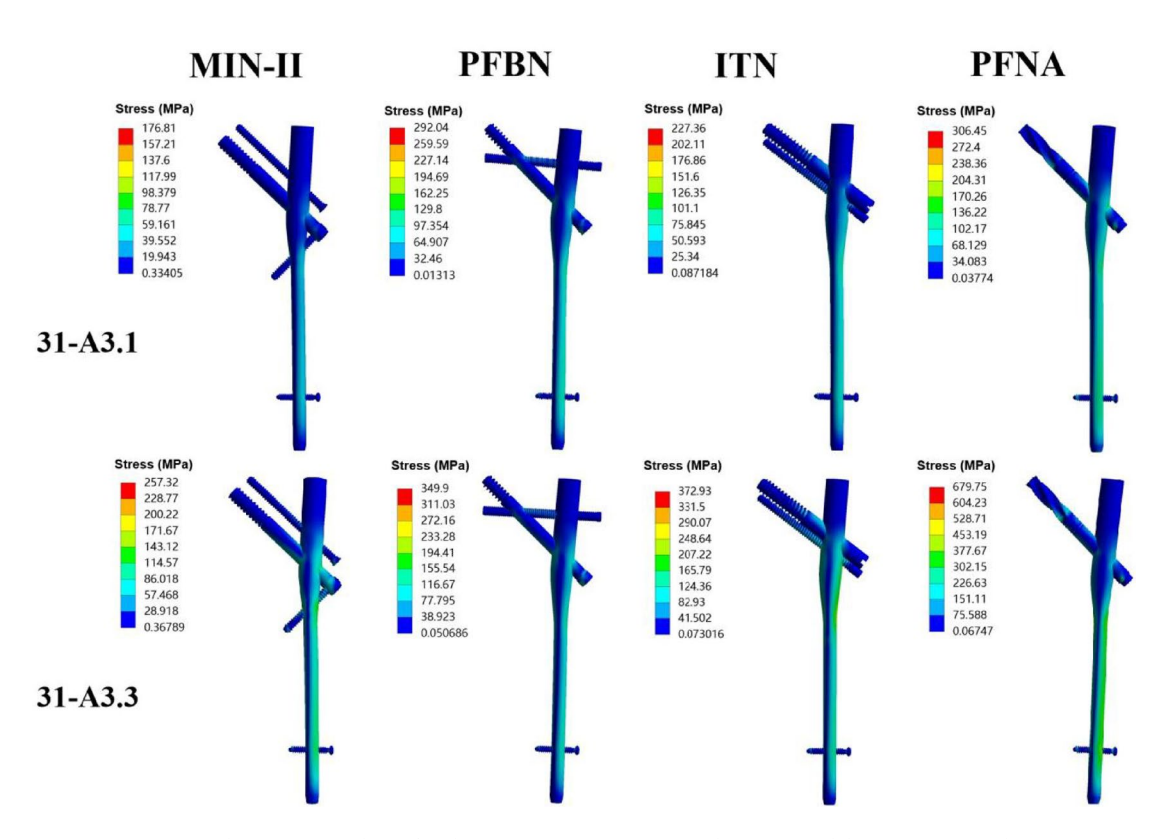


**Fig. 3.** Maximal VMS on implants for the MIN-II, PFBN, ITN, and PFNA models in 31-A3.1 and 31-A3.3 fractures. VMS represents von Mises stress. *MIN-II* modified intramedullary nail-II, *PFBN* proximal femoral bionic nail, *ITN* InterTAN nail, *PFNA* proximal femoral nail antirotation.

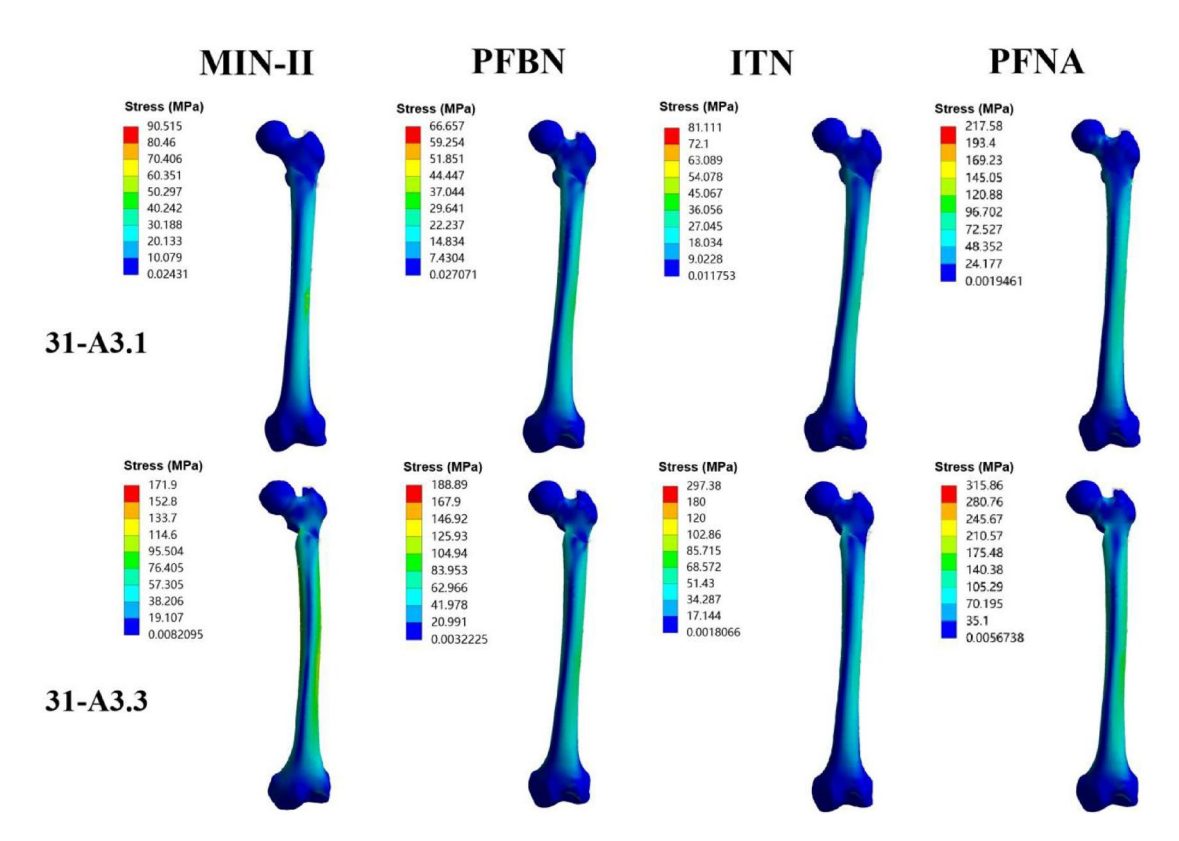


**Fig. 4.** Maximal VMS on bones for the MIN-II, PFBN, ITN, and PFNA models in 31-A3.1 and 31-A3.3 fractures. VMS represents von Mises stress. *MIN-II* modified intramedullary nail-II, *PFBN* proximal femoral bionic nail, *ITN* InterTAN nail, *PFNA* proximal femoral nail antirotation.

#### Discussion

In this research, we introduced a new cephalomedullary nail of MIN-II for managing ROT fractures. The biomechanical properties of four cephalomedullary nails (MIN-II, PFBN, ITN, and PFNA) were compared by finite element analysis. According to our results, the MIN-II displayed the best biomechanical performance, followed by PFBN, ITN and PFNA. Specifically, in comparison with the PFNA group, a 42.3–62.1% reduction was observed for maximal VMS on implants and a 45.6–58.4% reduction for maximal VMS on bones in the MIN-II group. For maximal displacement, the PD reduction was 20.2–30.0% in the MIN-II group, compared to the PFNA group. These data demonstrated that the design of MIN-II might be reasonable. Through decreasing stress concentration and enhancing mechanical stability, the MIN-II might be feasible in treating ROT fractures.

Currently, cephalomedullary nails have been used as the gold standard by most scholars for the treatment of femoral trochanteric fractures<sup>8,9,26</sup>. However, the failure rate of cephalomedullary fixation remains high for ROT fractures<sup>27–29</sup>. In Factor's study, 265 cases diagnosed as ROT fractures were managed with four kinds of cephalomedullary nails, including the Proximal Femoral Nail (PFN), Gamma3 nail, ITN, and the TFN-advanced proximal femoral nailing system (TFNA)<sup>27</sup>. The orthopedic complication (infection, cut-out, malunion, and nonunion) rate was 7.3–15.8% in three sub-types and the overall revision rate was 9.4%<sup>27</sup>. Hao et al. explored 45 patients with ROT fractures who accepted PFNA fixation<sup>28</sup>. Six (13.3%) experienced implant failure<sup>28</sup>. In Irgit's study, 148 patients with ROT fractures were fixed by cephalomedullary nails<sup>29</sup>. The complication rate was 12.2% while the revision rate was 8.1%<sup>29</sup>. The stress concentration and insufficient stability of cephalomedullary nails may be the key factors for the high failure rate in fixing ROT fractures. Conventional cephalomedullary nails have innovations in the number and structure of head screws. These modifications bring excellent biomechanical stability for those with femoral intertrochanteric fractures, such as the types of 31-A1 and 31-A2<sup>26,30</sup>. Nevertheless, for ROT fractures, also known as the type of 31-A3 in AO/OTA classification, current cephalomedullary nails are unable to provide satisfactory fixation effects.

Based on our results, compared with PFNA, ITN, and PFBN, the MIN-II presented the lowest maximal displacement and MDFS values. These data of our finite element study proved that the mechanical stability of MIN-II was good. Notably, a significant improvement has been made to the design of MIN-II, namely the introduction of the interlocking screw. This unique design may be the main reasons why the MIN-II exhibited such good biomechanical performance. Under axial loads, the proximal fracture fragment of ROT fractures will slide outward and downward while the distal femur will slide inward and upward<sup>31</sup>. Due to the head screws of PFNA and ITN being close to parallel to the main fracture line of ROT fractures, its ability to restrict the sliding of the fracture fragments is limited. Although the two proximal head screws of PFBN are interlocked, they are both located above the fracture line. The anti-sliding effects of PFBN are also limited to some extent. Unlike PFNA, ITN, and PFBN, the direction of the interlocking screw in MIN-II is close to perpendicular to the main

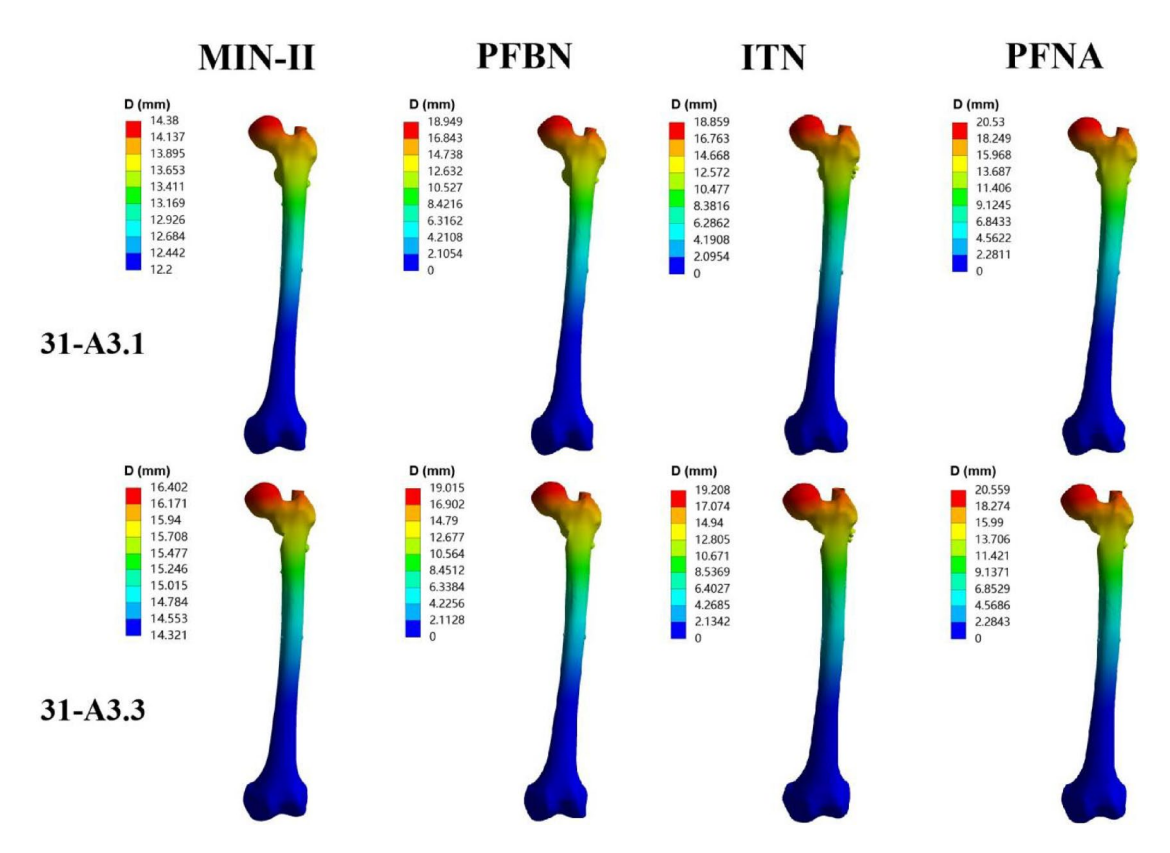


**Fig. 5.** Maximal displacement for the MIN-II, PFBN, ITN, and PFNA models in 31-A3.1 and 31-A3.3 fractures. *MIN-II* modified intramedullary nail-II, *PFBN* proximal femoral bionic nail, *ITN* InterTAN nail, *PFNA* proximal femoral nail antirotation.

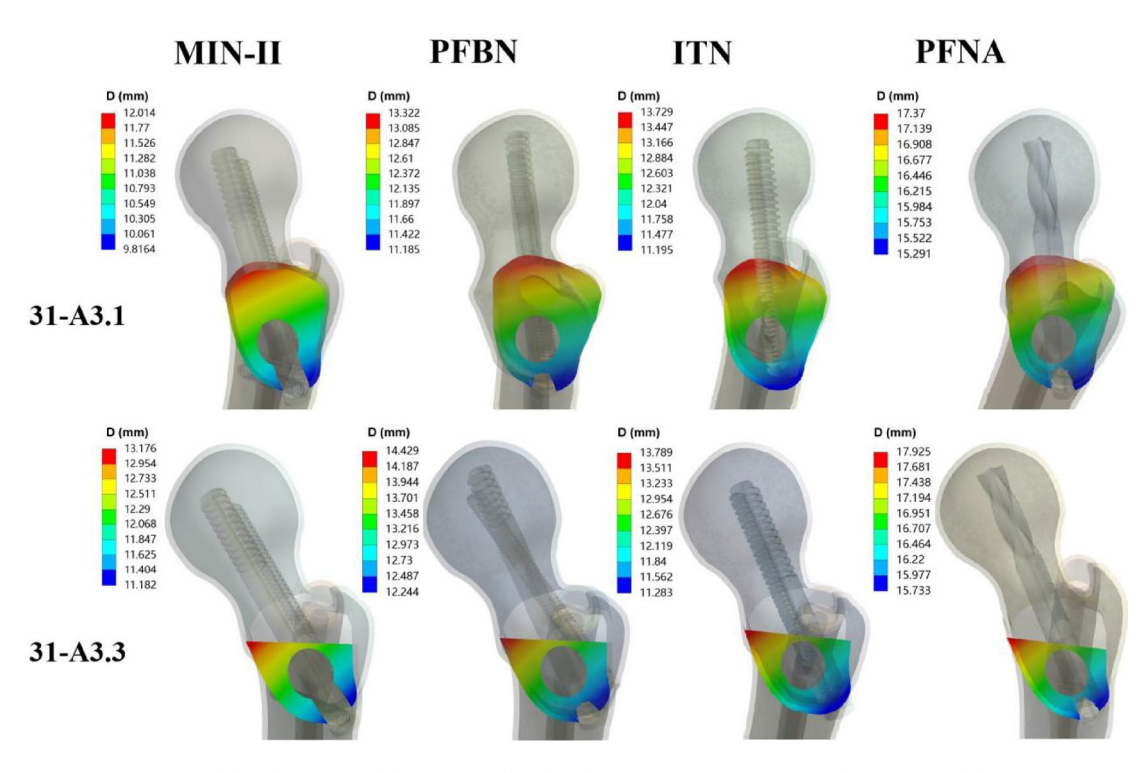


**Fig. 6.** Maximal displacement of fracture surface for the MIN-II, PFBN, ITN, and PFNA models in 31-A3.1 and 31-A3.3 fractures. *MIN-II* modified intramedullary nail-II, *PFBN* proximal femoral bionic nail, *ITN* InterTAN nail, *PFNA* proximal femoral nail antirotation.

fracture line of ROT fractures. From a geometric perspective, the screw perpendicular to the direction of the main fracture line has the greatest restriction on fracture fragment sliding. In addition, the interlocking screw and the lower head screw interlock with each other. The interlocking screw, the lower head screw, and the main nail form a small triangular stable structure. These structural features might provide superior stability for the fracture site of ROT fractures.

On the basis of our finite element data, compared to the PFNA, ITN, and PFBN fixation models, the MIN-II fixation model exhibited lower maximal VMS values on implants and femurs. The possible reasons are as follows. The junction between the main fracture line and the main nail is a stress concentration area of these fixation models. For PFNA, ITN, and PFBN, axial loads are transmitted along the main nail at the fracture line. Due to the introduction of the interlocking screw in MIN-II, the main fracture line of ROT fractures seems to be "locked" in the metal triangle structure. Near the fracture line of ROT fractures, a portion of axial loads is transmitted along the main nail towards the distal end. The other portion of axial loads is transmitted along the tail of the lower head screw to the interlocking screw, and then transmitted to the main nail and the distal end. This dual-line load conduction mode in ROT fractures might disperse local stress at the fracture site. The VMS stress data in our finite element analysis confirmed this point.

The design of MIN-II and PFN has some similarities. In the proximal part, both MIN-II and PFN have two head screws arranged in parallel. Compared to single-screw of PFNA and Gamma3 nail, dual-screw configuration helps to better resist rotation and provide axial support for ROT fractures. However, this proximal structure of PFN is prone to causing Z-effects or reverse Z-effects in axial load case<sup>32,33</sup>. The Z-effects refer to the displacement of the upper head screw towards the proximal end and its penetration into the acetabulum, while the lower head screw moves towards the distal end and causes this screw to retract. The reverse Z-effects indicate that the movement direction of the two head screws is opposite to that of the Z-effects. The possible complications caused by the Z-effects or reverse Z-effects may increase patients' pain and recovery time, and even significantly affect the therapeutic efficacy. Unlike PFN, the introduction of the interlocking screw in MIN-II restricts the sliding of the lower head screw. This may reduce the occurrence of Z-effects and reverse Z-effects, and finally decrease the fixation failure rate of implants.

There are some deficiencies of this research. Firstly, the material properties were assumed to be homogeneous, isotropic, and linear elastic, which was a simplification of the reality. Yet, to reduce interference factors, this simplification was essential in finite element studies. Secondly, our team only simulated vertical loads and did not simulate bending and torsional loads. In further research, we will explore the mechanical properties of MIN-II under bending and torsional loads. Thirdly, soft tissues were not simulated during model construction. Considering that the focus of this study was on the mechanical properties of MIN-II and its comparison with three other cephalomedullary nails, ignoring soft tissues can help us obtain accurate conclusions. Fourthly, before the MIN-II is ultimately used in patients with ROT fractures, its mechanical properties still need to be further explored through cadaver and clinical trials. We will improve these deficiencies in further research.

#### Conclusion

The modified intramedullary nail-II displayed the best biomechanical stability among the four cephalomedullary nails for the management of reverse obliquity trochanteric fractures. The introduction of the interlocking screw in MIN-II provided good anti-sliding effects via locking with the lower head screw. The MIN-II decreased local stress concentration by a dual-line load conduction mode in ROT fractures. Additionally, it may reduce the occurrence of Z-effects and reverse Z-effects via the introduction of the interlocking screw. Hence, the MIN-II might be a good option for patients with ROT fractures.

#### Data availability

The datasets analyzed during the current study are available from the corresponding author upon reasonable request.

Received: 21 March 2025; Accepted: 4 June 2025

Published online: 01 July 2025

#### References

- 1. Haidukewych, G. J., Israel, T. A. & Berry, D. J. Reverse obliquity fractures of the intertrochanteric region of the femur. *J. Bone Jt. Surg. Am.* 83, 643–650 (2001).
- Meinberg, E. G., Agel, J., Roberts, C. S., Karam, M. D. & Kellam, J. F. Fracture and dislocation classification compendium-2018. J. Orthop. Trauma 32, S1–S10 (2018).
- 3. Park, S. Y., Yang, K. H., Yoo, J. H., Yoon, H. K. & Park, H. W. The treatment of reverse obliquity intertrochanteric fractures with the intramedullary hip nail. *J. Trauma* 65, 852–857 (2008).
- 4. Mears, S. C. & Kates, S. L. A guide to improving the care of patients with fragility fractures, edition 2. *Geriatr. Orthop. Surg. Rehabil.* 6(2), 58–120 (2015).
- 5. Ablett, A. D. et al. Cephalomedullary nailing for subtrochanteric and reverse-oblique femoral fractures: Comparison of a single versus dual lag screw device. *J. Bone Jt. Surg. Am.* **107**(4), 389–396 (2025).
- 6. Yamanaka, T., Matsumura, T., Ae, R. & Takeshita, K. AO/OTA 31A3 fractures and postoperative complications in older patients. *J. Orthop. Sci.* 29(4), 1073–1077 (2024).
- 7. Şensöz, E., Ergun, S., Kayaalp, M. E. & Eceviz, E. The comparison of dynamic condylar screw plate to proximal femoral nail in reverse oblique and transverse intertrochanteric fractures: A retrospective study on 61 patients. *Cureus* 15(3), e36397 (2023).
- 8. Tai, D., Chou, S., Taylor, A. M. & Moran, C. G. Reverse oblique intertrochanteric femoral fractures treated with the intramedullary hip screw (IMHS). *Injury* 43, 817–821 (2012).
- 9. Matre, K. et al. Sliding hip screw versus IM nail in reverse oblique trochanteric and subtrochanteric fractures. A study of 2716 patients in the Norwegian Hip Fracture Register. *Injury* 44, 735–742 (2013).

- Wang, Y. et al. Finite element analysis of proximal femur bionic nail (PFBN) compared with proximal femoral nail antirotation and InterTan in treatment of intertrochanteric fractures. Orthop. Surg. 14(9), 2245–2255 (2022).
- 11. Fu, H. et al. A comparative study of the early postoperative outcome of three intramedullary fixation modalities in the treatment of intertrochanteric fractures of the femur in the elderly. J. Musculoskelet. Neuronal. Interact. 24(3), 310–317 (2024).
- 12. Yang, Y. J. et al. Comparative study of a novel proximal femoral bionic nail and three conventional cephalomedullary nails for reverse obliquity intertrochanteric fractures: A finite element analysis. Front. Bioeng. Biotechnol. 12, 1393154 (2024).
- 13. Xiong, C. et al. Finite element analysis of proximal femoral bionic nail (PFBN), proximal femoral nail antirotation and InterTan for treatment of reverse obliquity intertrochanteric fractures. *Orthop. Surg.* 17(3), 888–899 (2025).
- 14. Hantouly, A. T. et al. The role of cerclage wiring in the management of subtrochanteric and reverse oblique intertrochanteric fractures: A meta-analysis of comparative studies. Eur. J. Orthop. Surg. Traumatol. 33(4), 739–749 (2023).
- 15. Wang, C. F. et al. Biomechanical evaluation of a modified intramedullary nail for the treatment of unstable femoral trochanteric fractures. *Heliyon* **10**(8), e29671 (2024).
- 16. Abdul Wahab, A. H., Wui, N. B., Abdul Kadir, M. R. & Ramlee, M. H. Biomechanical evaluation of three different configurations of external fixators for treating distal third tibia fracture: Finite element analysis in axial, bending and torsion load. *Comput. Biol. Med.* 127, 104062 (2020).
- 17. Li, M. et al. Three dimensional mapping of intertrochanteric fracture lines. Chin. Med. J. Engl. 132(21), 2524-2533 (2019).
- 18. Machado, M. M., Fernandes, P. R., Zymbal, V. & Baptista, F. Human proximal femur bone adaptation to variations in hip geometry. *Bone* 67, 193–199 (2014).
- 19. McCartney, W., MacDonald, B., Ober, C. A., Lostado-Lorza, R. & Gómez, F. S. Pelvic modelling and the comparison between plate position for double pelvic osteotomy using artificial cancellous bone and finite element analysis. *BMC Vet. Res.* 14(1), 100 (2018).
- Huang, Q. et al. Biomechanical evaluation of two modified intramedullary fixation system for treating unstable femoral neck fractures: A finite element analysis. Front. Bioeng. Biotechnol. 11, 1116976 (2023).
- Li, J. T. et al. Finite element analysis of different configurations of fully threaded cannulated screw in the treatment of unstable femoral neck fractures. J. Orthop. Surg. Res. 13(1), 272 (2018).
- Xia, Y. et al. Biomechanical study of two alternative methods for the treatment of vertical femoral neck fractures—A finite element analysis. Comput. Methods Programs Biomed. 211, 106409 (2021).
- 23. Zhang, Y. et al. Biomechanical evaluation of the expansive cannulated screw for fixation of femoral neck fractures. *Injury* **42**(11), 1372–1376 (2011).
- 24. Lewis, S. R. et al. Surgical interventions for treating extracapsular hip fractures in older adults: a network meta analysis. *Cochrane Database Syst. Rev.* 2(2), CD013405 (2022).
- 25. Papini, M., Zdero, R., Schemitsch, E. H. & Zalzal, P. The biomechanics of human femurs in axial and torsional loading: Comparison of finite element analysis, human cadaveric femurs, and synthetic femurs. *J. Biomech. Eng.* 129(1), 12–19 (2007).
- 26. D'Arrigo, C. et al. Intertrochanteric fractures: Comparison between two different locking nails. Int. Orthop. 36, 2545–2551 (2012).
- Factor, S. et al. Intertrochanteric (reverse oblique) fracture subclassifications AO/OTA 31-A3 have no effect on outcomes or postoperative complications. Clin. Orthop. Surg. 16(2), 194–200 (2024).
- 28. Hao, Y. L. et al. Risk factors for implant failure in reverse oblique and transverse intertrochanteric fractures treated with proximal femoral nail antirotation (PFNA). J. Orthop. Surg. Res. 14(1), 350 (2019).
- Irgit, K. et al. Reverse oblique and transverse intertrochanteric femoral fractures treated with the long cephalomedullary nail. J. Orthop. Trauma 29(9), e299-304 (2015).
- 30. Yang, F., Li, X., Zhao, L. & Yang, Q. Dual-screw versus single-screw cephalomedullary nails for intertrochanteric femoral fractures: A systematic review and meta-analysis. *J. Orthop. Surg. Res.* 18(1), 607 (2023).
- 31. Haidukewych, G. J. Nonunion of fractures of the subtrochanteric region of the femur. Tech. Orthop. 23(2), 131-136 (2008).
- 32. Al-yassari, G., Langstaff, R. J., Jones, J. W. & Al-Lami, M. The AO/ASIF proximal femoral nail (PFN) for the treatment of unstable trochanteric femoral fracture. *Injury* 33, 395–399 (2002).
- 33. Yoo, J. H. et al. The results of proximal femoral nail antirotation: A comparative study with proximal femoral nail. *J. Korean Hip Soc.* 20, 286–292 (2008).

#### Author contributions

K.Z. designed the study. Q. W., Y. L, L. L., T. M., Z. L., K. Z. and Q. H. searched relevant clinical data, analyzed and interpreted the data. Q. W. wrote the manuscript. Q. H. and K. Z. contributed most in the revision of this manuscript. All authors have approved the final version of the manuscript.

#### Funding

This study was supported by the Bureau project of Xi'an Health Commission (2024ms08). The funding source has no role in study design, conduction, data collection or statistical analysis.

#### **Declarations**

#### Competing interests

The authors declare no competing interests.

#### Consent to participate/consent to publish

All patients or their family members have signed the informed consent before surgery and provided the consent to publish and report individual clinical data.

#### Additional information

**Correspondence** and requests for materials should be addressed to K.Z. or Q.H.

Reprints and permissions information is available at www.nature.com/reprints.

**Publisher's note** Springer Nature remains neutral with regard to jurisdictional claims in published maps and institutional affiliations.

Open Access This article is licensed under a Creative Commons Attribution-NonCommercial-NoDerivatives 4.0 International License, which permits any non-commercial use, sharing, distribution and reproduction in any medium or format, as long as you give appropriate credit to the original author(s) and the source, provide a link to the Creative Commons licence, and indicate if you modified the licensed material. You do not have permission under this licence to share adapted material derived from this article or parts of it. The images or other third party material in this article are included in the article's Creative Commons licence, unless indicated otherwise in a credit line to the material. If material is not included in the article's Creative Commons licence and your intended use is not permitted by statutory regulation or exceeds the permitted use, you will need to obtain permission directly from the copyright holder. To view a copy of this licence, visit <a href="http://creativecommons.org/licenses/by-nc-nd/4.0/">http://creativecommons.org/licenses/by-nc-nd/4.0/</a>.

© The Author(s) 2025